A Lumped-Circuit Study of Basic Oscillator Behavior

By N. D. KENYON

(Manuscript received August 27, 1969)

This paper presents an experimental study of the oscillations set up in a circuit consisting of a negative conductance and a multiple-resonant load. Its purpose was to verify that such a circuit can account for many of the irregular phenomena commonly observed during tuning of practical microwave solid-state oscillators; such effects as discontinuous frequency changes, low circuit Q-factors, power variations, spurious oscillations and noise conditions are all readily reproduced in a simple low-frequency analogue. There is close correspondence with a first-order analysis.

I. INTRODUCTION

In the course of routine locking-bandwidth measurements on IMPATT diodes in the 50–60 GHz range, some observations were made that could not be accounted for by the simple theory[1–4] of injection locked oscillators. In particular, locking ranges of about 100 MHz for −40 dB injected power were measured, indicating an extremely low effective circuit Q-factor (≈ 5). In addition this range was asymmetrical about the free-running frequency, and was not exactly proportional to the injected voltage. On occasions there was at one end of the locking range a hysteresis between locking and unlocking conditions.

Other phenomena commonly observed during tuning experiments on solid-state oscillators include the following:

(*i*) A discontinuous change in frequency (here referred to as a "jump") as a parameter is varied (bias current, perhaps, or a tuning stub). If the tuning is reversed the jump occurs at a displaced frequency ("hysteresis").

(*ii*) In the neighborhood of a jump, the hitherto single line spectrum may acquire sidebands at displacements of order 0.1 to 1 percent.

(*iii*) Under some circuit conditions a broadband noisy output may be obtained.

To explain these effects the passive circuit "seen" from the diode terminals must be treated as more complex than the simple resonant circuit normally assumed. Kurokawa[5] has analyzed the case in which the active element is as simple as possible, but is connected to a passive load impedance of general form $Z(\omega)$; it is found that most of the observations can be accounted for by ascribing certain patterns to the locus $Z(\omega)$. The conditions are summarized in Section II.

Since the form of $Z(\omega)$ for a packaged diode in a waveguide structure can be very complicated, is difficult to determine precisely, and more difficult still to design, a lumped-circuit approach at low frequency was used to verify the theoretical predictions. The frequency of 350 kHz was chosen so that measurements would be relatively unhindered by stray capacitance effects, but that spectra could be analyzed with sufficient resolution.

II. SUMMARY OF ANALYTICAL PREDICTIONS

When a negative conductance $-\bar{G} + j\bar{B}$ is connected to a load $G + jB$, the voltage amplitude A and frequency ω of the resulting equilibrium oscillation are determined by

$$\bar{G}(A) = G(\omega) \tag{1a}$$

$$-\bar{B}(A) = B(\omega). \tag{1b}$$

These equations define the intersections in the complex impedance plane of the loci $\bar{G}(A) - j\bar{B}(A) = -\bar{Y}$ and $G(\omega) + jB(\omega) = Y(\omega)$, these being referred to as the "device line" and "load line" respectively. For a single-tuned parallel-resonant circuit, $Y(\omega)$ is a straight vertical line; for multiple-tuned circuits it may acquire bends and loops. From Kurokawa's analysis of the latter situation, the following predictions emerge:

(*i*) Let θ be defined as in Fig. 1. Stable oscillation at the point P is only possible if $0 < \theta < \pi$. Moreover, whenever the condition $\theta \to 0$ obtains, the noise of the oscillations will greatly increase.

(*ii*) In Fig. 2, the line PT is the device line or, if that is not straight, PT is the tangent to the device line at P. The point T lies on a line drawn through the frequency points $\omega_0 \pm \Delta\omega$ on the load line. If the resistive component G' of PT satisfies

$$G' = -\tfrac{1}{2}A_0 \frac{\partial \bar{G}}{\partial A}$$

then spurious oscillations will grow at $\omega_0 \pm \Delta\omega$. If spurious oscillations

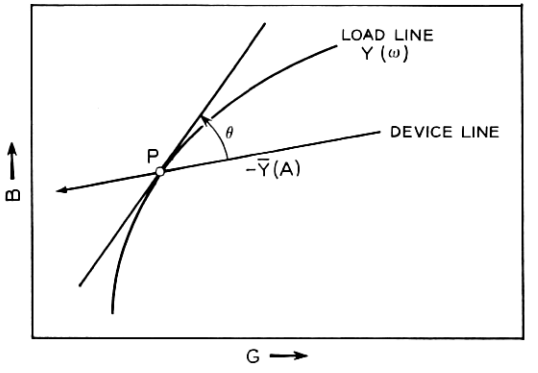

Fig. 1 — Definition of θ at oscillation point.

are not small, the values of ω_0 , A_0 , and so on will be affected, and the first order condition above will not apply.

(*iii*) Figure 3 shows an injected signal of small amplitude a_0 at a frequency ω_s close to, but not coincident with, the intersection of device and load lines at ω_0 . The perpendicular d is constructed from ω_s to the device line (which is here assumed straight); locking occurs if the length of d is not greater than a_0/A_0 . There are additional requirements for stability of locked oscillation, the principal one being that the angle β be less than $\pi/2$.

(*iv*) The relationship between injected current, oscillation amplitude and locking range for a near-horizontal device line ($\partial\bar{B}/\partial\bar{G} \simeq 0$) is determined by $| \Delta B | = a_0/A_0$, ΔB being the susceptance change from ω_0 to unlocking frequency. Thus if a_0 and A_0 are held constant the ex-

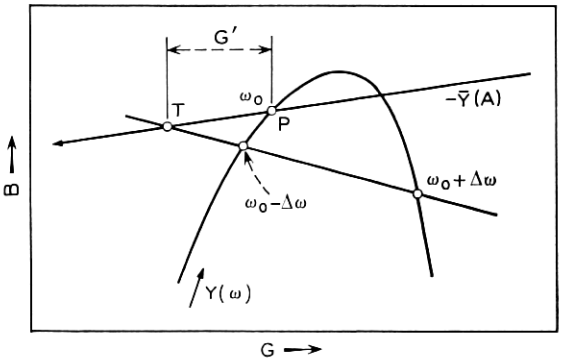

Fig. 2 — Definition of G′ for spurious sidebands.

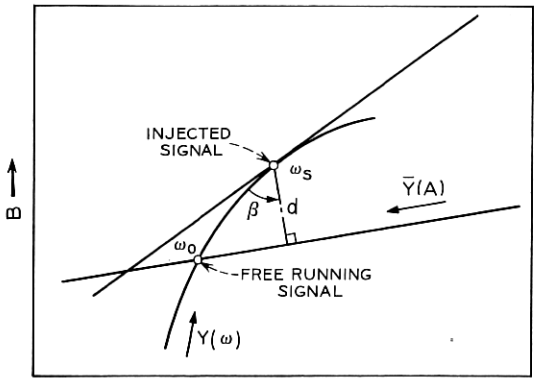

Fig. 3 — Injection locking conditions.

tremities of the locking range will be those for which $B(\omega) - B(\omega_0) = \pm a_0/A_0$.

If the device line is not horizontal, but has a small gradient g, then ΔB must be corrected by the factor $(1 - g\ \Delta G/\Delta B)$.

(*v*) The theory can be applied equally well to the case of a negative impedance $-\bar{R}(A) + j\bar{X}(A)$ simply by reading current for voltage and vice versa, and substituting R, X, Z, and so on, for G, B, Y. The circuit used must then of course have large impedance far from resonance, to inhibit undesired oscillation.

III. ACTIVE ELEMENTS

Both negative conductances and negative resistances were used, taking the circuit forms shown in Fig. 4. The negative conductance is

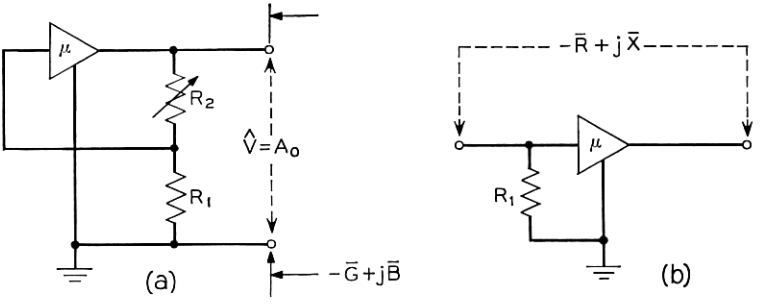

Fig. 4 — Negative admittance and impedance circuits.

readily seen to be

$$\bar{Y} = \frac{-\mu R_1 + (R_1 + R_2 + R_3)}{(R_1 + R_2)R_3}$$

where R_3 is the amplifier output impedance and μ the voltage gain. If there is a phase shift $(2n\pi + \varphi)$ across the amplifier, this equation contains a complex μ:

$$\mu = \mu_0(1 + j\varphi)$$

which introduces an imaginary component $\bar{B}$ into $\bar{Y}$. The amplitude A of oscillation depends on the saturation behavior of the amplifier $\mu(A)$: as A grows, $\mu(A)$ (and therefore $\bar{G}$) declines until the equilibrium condition (1a) is established. At the same time the frequency settles such that the total circuit susceptance is zero (1b).

The theory leading to the predictions of Section II assumes that the device characteristic $\bar{Y}(A)$ is independent of frequency. This is so here if $\mu(A)$ is not frequency dependent and the circuit is free of parasitic capacitance.

The negative impedance of Fig. 4(b) is

$$\bar{Z} \cong -\mu R_1 + R_3 .$$

By making R_1 low, $\bar{Z}$ is confined to a few hundred ohms. The behavior of $\bar{Z}(A)$ is very similar to $\bar{Y}(A)$ above, but the circuit has the disadvantage that no point in the oscillating loop can be grounded; thus large errors arose when injection-locking characteristics were measured. We confine our attention here to the negative admittance circuit.

IV. METHOD OF MEASUREMENT

The amplifier used was a C-Cor 1319F transistor video amplifier, with a small signal gain of 40 dB into 50 ohms, and a bandwidth of 15 MHz. The characteristic $\bar{Y}(A)$ for a given feedback resistor was established by direct measurement, not by calculation from μ, R_1, R_2, R_3.

Figure 5 shows schematically the essentials of the experiment. Apart from the active $\bar{Y}$ and passive $Y(\omega)$ networks, there is an oscilloscope, an injection signal source, a monitoring circuit for the frequency spectrum, and a bridge for passive admittance measurements on $Y(\omega)$.

Monitoring equipment is hung on to a current pick-up lead, which has a negligible loading effect on the circuit. From a counter the frequency is known to 0.01 kHz, oscillations usually being stable to this degree. The wave analyzer determines to the same accuracy the fre-

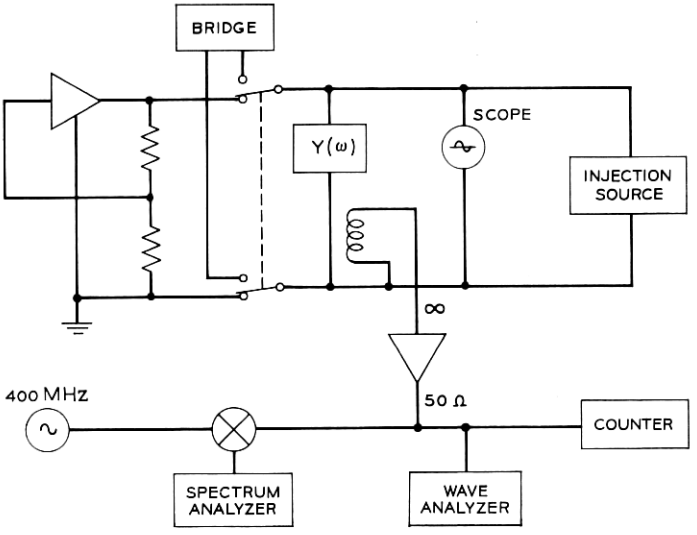

Fig. 5 — Schematic of low-frequency experiment.

quency of sidebands. Finally a convenient display of the spectrum is provided by up-converting into a spectrum analyzer.

To make passive measurements the negative admittance was removed and the RF bridge connected by a short cable to the points shown. The wave analyzer was employed as a very sensitive null detector (to −90 dB).

The arrangement of Fig. 6 was convenient for giving an oscilloscope display of the admittance.

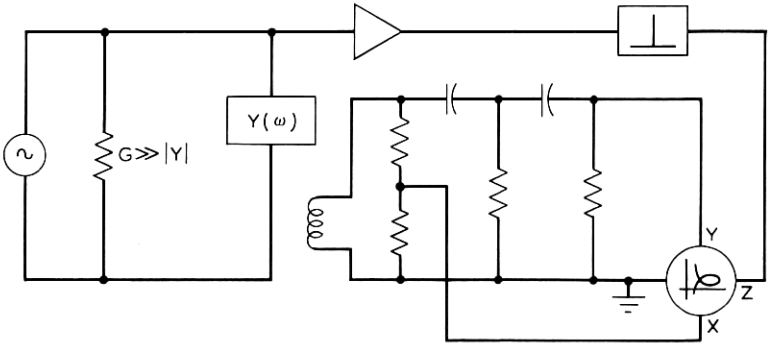

Fig. 6 — Admittance display circuit.

The oscilloscope beam is driven in a circular path of radius proportional to the current through $Y(\omega)$. The spot is brightened by a 2 ns pulse at the instant of maximum voltage. The ac voltage amplitude is approximately constant. The circuit is obviously of limited bandwidth and was not used for quantitative measurements.

V. MEASUREMENTS

5.1 *Characterization*

The device line $-\bar{Y}(A)$ was established from oscillations with a single-tuned parallel-resonant circuit (Fig. 7, inset). Since the imaginary component $\bar{B}$ was small, the frequency was close to the resonant frequency, and the latter was varied by changing L. The oscillation frequency ω_0 and amplitude A were measured, and then the bridge was used to determine the admittance $Y(\omega_0)$: this quantity is plotted di-

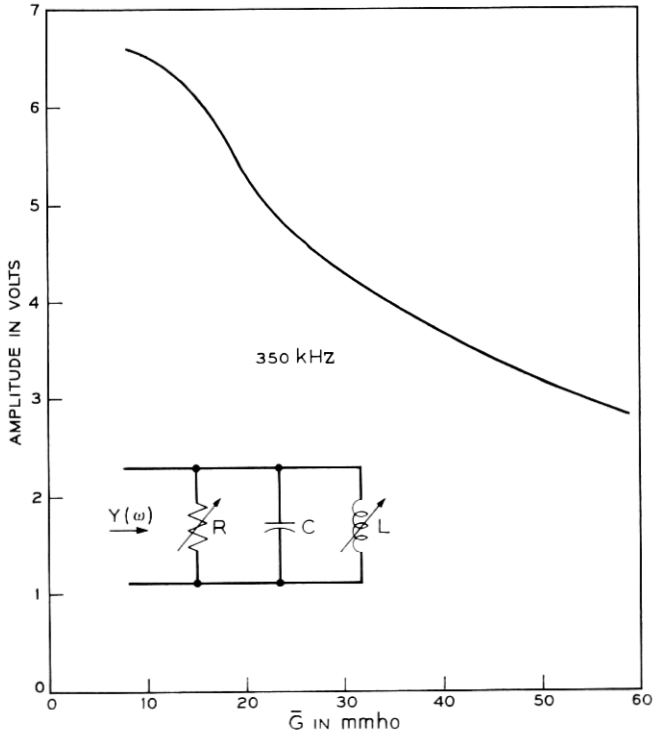

Fig. 7 — Conductance saturation curve at **350 kHz**.

rectly as the device line, since $-\bar{Y}(A) = \bar{Y}(\omega_0)$ at equilibrium. Figure 7 gives the conductance-saturation characteristic at 350 kHz, these amplitude points being then superposed on the device line plot of Fig. 8. The variation of these characteristics over the range 310–390 kHz were found to be quite small. The device line is seen to be neither steep nor sharply curved: thus, the negative admittance is a good approximation to the idealized one assumed in the analysis.[5]

It may be worth noting at this point that tuning of the shunt inductance L is roughly equivalent to a complete vertical displacement of the locus $Y(\omega)$ in the complex admittance plane. The device line in this experiment remains stationary, and the frequency of oscillation and amplitude vary according to the changing point of intersection. However similar phenomenological observations are to be expected if it is the device line that undergoes a vertical displacement—this commonly occurs for bias current changes of solid-state microwave sources. In succeeding paragraphs it is assumed that only the relative vertical relationship of device and load lines is significant, and that this can be changed at will by tuning of L.

5.2 *Double Resonant Circuit*

The addition of a series resonant circuit L_2, C_2, R across the parallel L_1, C_1 provides a number of interesting situations (Figs. 9, 11, 13). The resonant frequency is the same for both circuits.

Defining $Q_1 = \omega_0 C_1 R$, $Q_2 = \omega_0 L_2/R$, and $b = B/R$, we have

$$\partial b/\partial\omega\,|_{\omega_0} = 2C_1R - 2L_2/R = (2/\omega_0)(Q_1 - Q_2).$$

The susceptance of the series circuit tends to compensate that of the original parallel circuit in the neighborhood of resonance, and the combination becomes broader band than either of the two; the effective

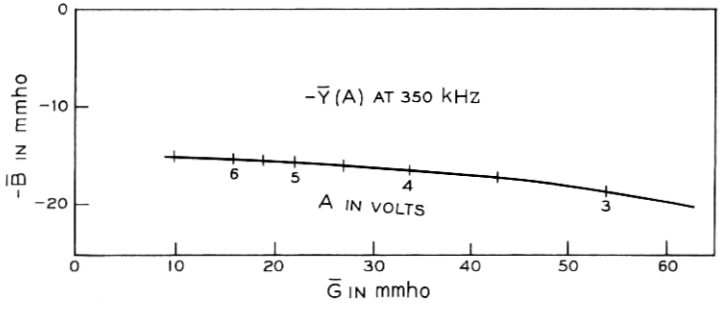

Fig. 8 — Device line plot at 350 kHz.

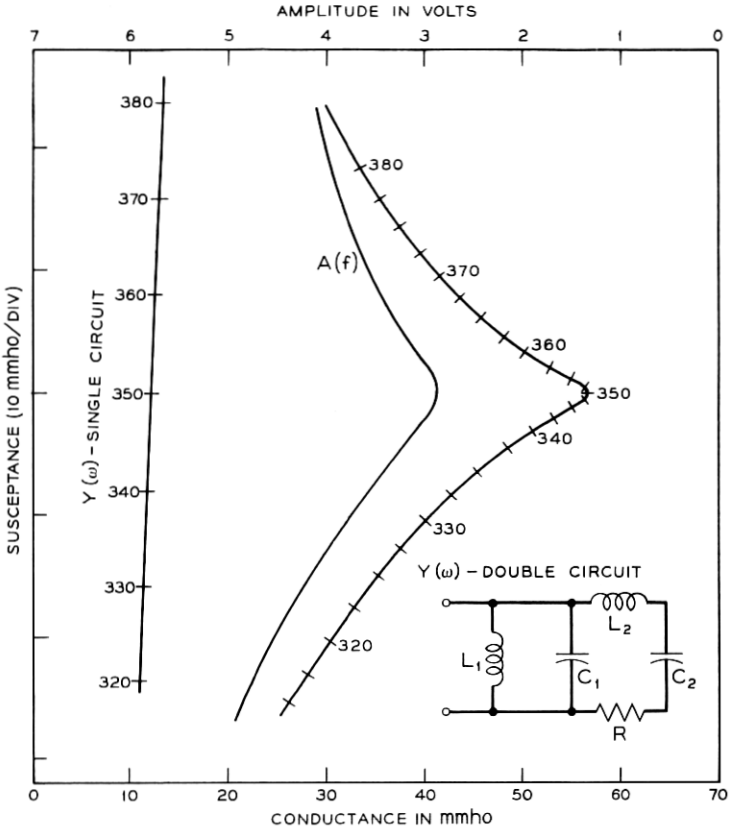

Fig. 9 — Double-tuned circuit behaviour.

Q at ω_0 is the difference $Q_1 - Q_2$, which may obviously be made as low as desired. We shall consider in turn the three cases $Q_1 > Q_2$, $Q_1 = Q_2$, $Q_1 < Q_2$.

5.2.1 *Case 1:* $Q_1 > Q_2$

Figure 9 shows a typical measured $Y(\omega)$ locus for this case. We impose the further condition that at no point is the device line steeper than this load line so that the requirement $0 < \theta < \pi$ (See i in Section II) is met. The measured amplitude at each frequency is also plotted in Fig. 9, and corresponds to the appropriate points of the device characterization, including the general decline with increasing frequency. By comparison with the single-resonant case the frequency points are

relatively crowded at the center of the locus, and there is considerable variation of G in this region. When this circuit is connected to the device, the oscillations generated vary continuously in frequency and amplitude as L_1 is tuned, and there are no unstable points.

The small-signal locking behavior of this kind of circuit was investigated. A variable-frequency source of constant short-circuit current (5 mA peak) injected a driving signal into the terminals of $\bar{Y}$ (See Fig. 6). Oscillation amplitude at 350 kHz was determined, together with the frequencies ω_1, ω_2 at which the oscillator fell out of synchronism with the driver. Then the negative admittance was removed, and the change of susceptance $2\Delta B$ of the passive circuit between ω_1 and ω_2 was accurately determined (by the addition of known capacitances across the terminals to maintain bridge balance). This procedure was repeated for various $(Q_1 - Q_2)$ by changing R.

The results appearing in Table I show good consistency of ΔB with a/A, except for the last two cases. These have critically low Q and the locking phenomenon is affected by excessive noise and drifting. Figure 10 shows susceptance and frequency ranges as a function of injected current level for a particular value of R and A. The $\Delta B - a$ relationship is linear, as expected, while the locking range falls off at higher levels. Over the linear region the voltage-gain $\times$ fractional-bandwidth product is constant, as for a single-tuned circuit, namely,

$$g \times b = 2/(Q_1 - Q_2).$$

We have thus confirmed that the locking range of an oscillator for a specific circuit is $\omega_1 - \omega_2$, where

$$| B(\omega_1) - B(\omega_2) | = 2a/A.$$

[For microwave circuits the right-hand side would be better expressed

TABLE I

$2\Delta f$ (kHz)	A (Volts)	a/A (mmho)	ΔB (mmho)	
1.95	5.8	0.85	0.82	
2.6	5.3	0.94	0.96	
3.6	4.9	1.02	1.05	
5.5	4.7	1.08	1.08	
7.1	4.6	1.08	1.10	
9.7	4.5	1.12	1.06	
16.6	4.5	1.11	0.99	$(Q_1 = Q_2)$
19.0	4.5	1.11	0.94	$(Q_1 < Q_2)$

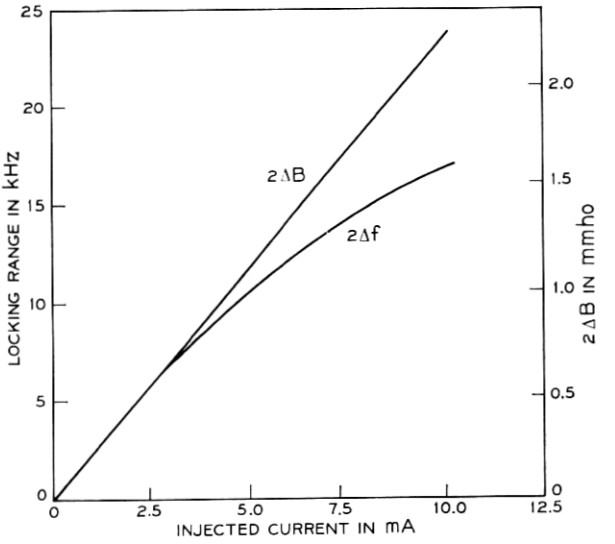

Fig. 10 — Locking range vs. driving signal in broadband circuit.

as $(4/R)(P_i/P_0)^{\frac{1}{2}}$, where P_0 is the output power and P_i the available driver power.] Moreover the combination of two tuned circuits of similiar Q can give a very low effective Q and correspondingly large locking gain-bandwidth product.

5.2.2 *Case 2:* $Q_1 \cong Q_2$

Under this condition a cusp appears on the admittance locus: Fig. 11(a) compares this with the $Q_2 = 0$ case (—markers are at 5 kHz

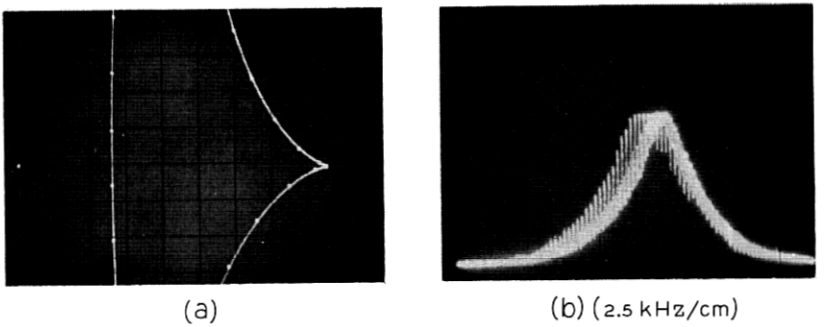

Fig. 11 — Circuit admittance for $Q_2 = 0$ and $Q_2 = Q_1$ cases.

intervals). Oscillations right at the point of the cusp are very noisy (Fig. 11b). When Q_1 is slightly greater than Q_2, the load line may be parallel to the device line ($\theta = 0$) over a considerable band, and the extremely noisy broadband output results (Fig. 12).

5.2.3 *Case 3:* $Q_2 > Q_1$

A loop appears in the admittance locus (Fig. 13a). Part *i* in Section II states that if the device line has the slope indicated by the dotted line, the region between the points A and C (at which the device line would be tangent) has $0 > \theta > -\pi$ and is therefore unstable. As the

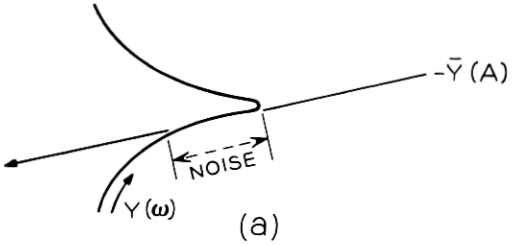

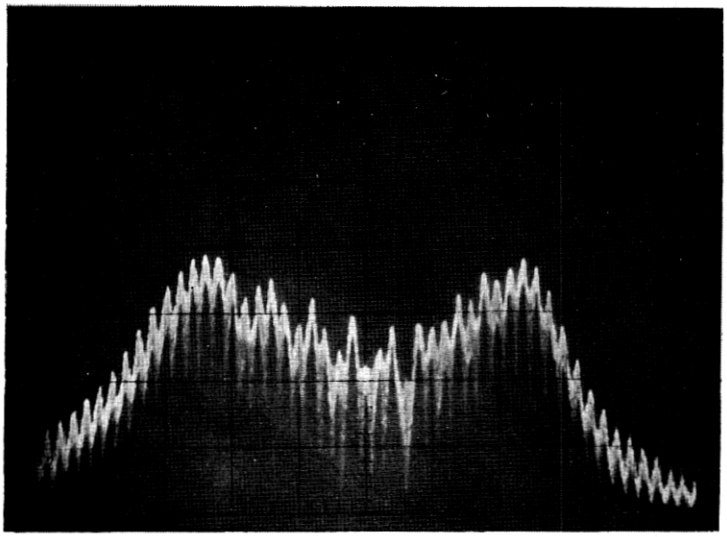

(b) (5 kHz/cm)

Fig. 12 — Broadband noise conditions.

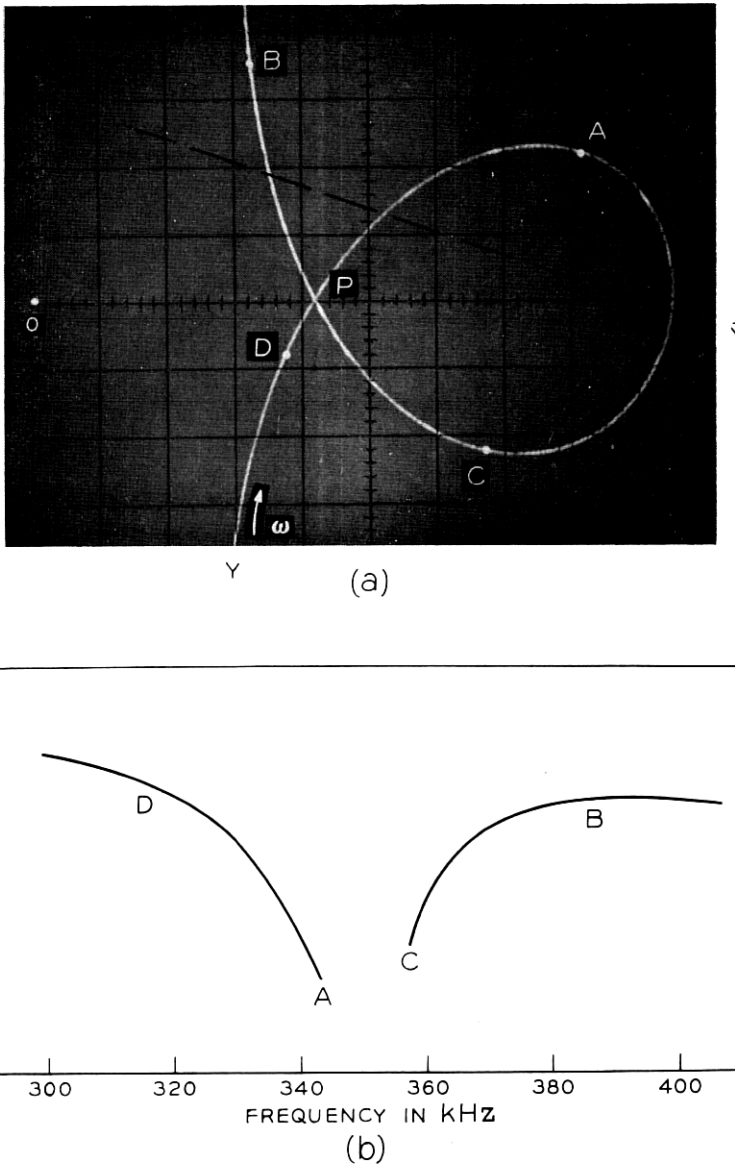

Fig. 13 — Admittance loop for $Q_2 > Q_1$.

circuit is tuned (by decreasing L_1) the frequency moves through D to A, at which it jumps to B; tuning the other way, the frequency moves down to C, then jumps further down still to D. Fig. 13(b) shows the behavior of the amplitude. There are two regions of overlap DA, BC in which oscillation is entirely stable at either of two points, depending on the way in which this oscillation was set up. By accurate measurements of the slope of $Y(\omega)$ at the jump frequencies, and the slope $\partial\bar{B}/\partial\bar{G}$ of the device line at the appropriate values of A and f, it was established that the jumps AB and CD occurred very close to the points of tangency of the device line to the $Y(\omega)$ locus.

If a large parallel conductance G_p is added to $Y(\omega)$, all oscillation ceases (Fig. 14). Reduction of G_p is now equivalent to a leftward displacement of $Y(\omega)$; at the dotted position oscillation of low amplitude is initiated. Clearly this oscillation can never begin at any point on the loop, except the cross-over point P. If a low-amplitude signal is initiated at P, it is possible for the spectrum to contain both frequencies, though usually one will predominate.

5.3 *Spurious Oscillations*

The condition of part *ii* in Section II requires that the line joining points $\omega_0 \pm \Delta\omega$ should intersect the tangent to the device line through ω_0 at a point to the *left* of A_0. Considering Fig. 15(a) (shaded part unstable) we see that for the double-resonant circuit such intersections invariably occur to the *right*. In practice, noisy sidebands were only observed in such a circuit when the device-line had been given a sharp curvature.

Figure 15(b) shows that the sideband condition will be fulfilled if

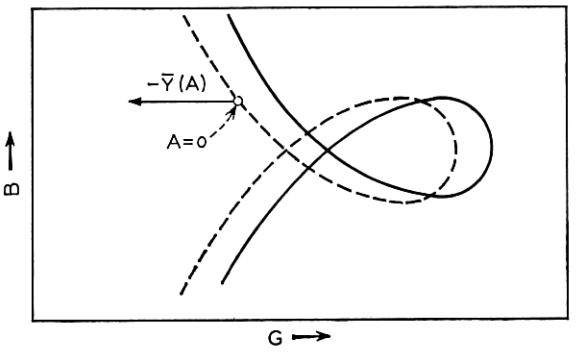

Fig. 14 — Signal initiation.

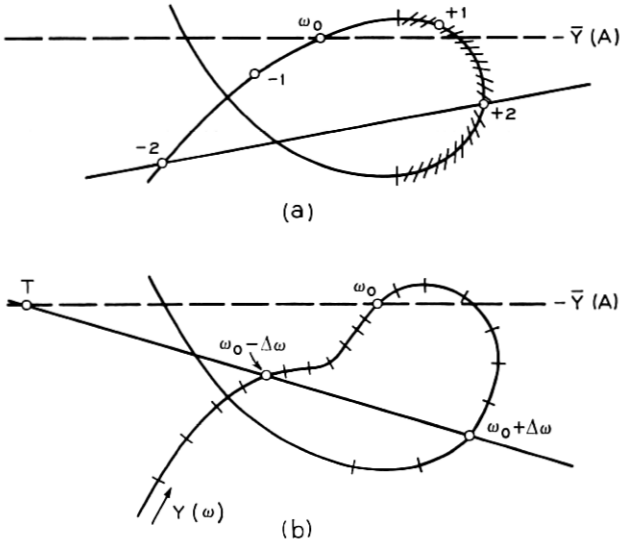

Fig. 15 — Spurious sideband conditions.

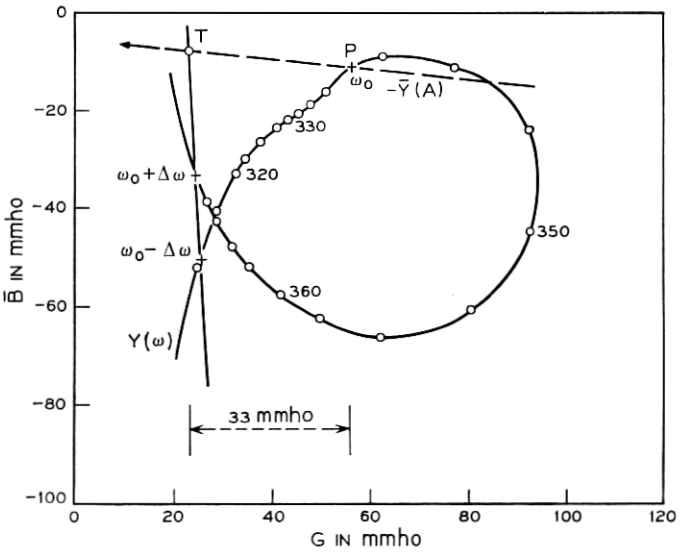

Fig. 16 — Sideband measurements.

the frequency points to the left of ω_0 can be crowded together. This was achieved by the addition of another series resonant circuit of intermediate Q and tuned to about 330 kHz. It was then very easy to get spurious sidebands over an appreciable range of frequencies. A typical case is shown in Fig. 16. As L_1 is reduced the frequency climbs to 343.5 and jumps to 380; between 340 and 343.5 there are noise sidebands, beginning at 340 with very small amplitude, progressing through greater amplitudes and additional sidebands at $\omega_0 \pm n\Delta\omega$; before the jump, the first sidebands were almost the same amplitude as the principal oscillation, and interstitial components at $\omega_0 \pm n\Delta\omega/2$ and so on also appeared (Fig. 17).

Accurate measurements were made in the case of very small sidebands, for which the small signal theory may be expected to apply. In Fig. 16 the admittance $Y(\omega)$ is shown accurate to within 1 mmho (relatively) on each scale. The line through $\omega_0 \pm \Delta\omega$ is thus subject to little uncertainty. The measured device-line slope at ω_0 gives an

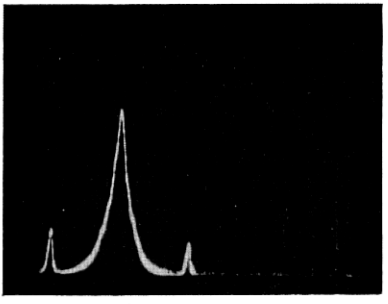

(a) 339.7 kHz

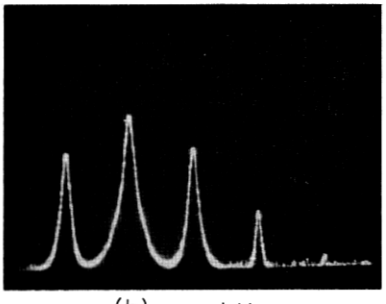

(b) 341.5 kHz

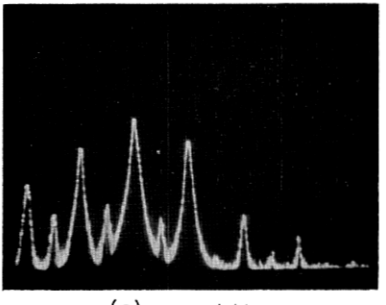

(c) 343.5 kHz

Fig. 17 — Oscillation spectra.

intersection at T as shown, and PT $\cong$ 33 mmho; the measured value of $(-\frac{1}{2}A_0\ \partial\bar{G}/\partial A)$ was 39 mmho, indicating that the intersection should have been more to the left. Other similar measurements gave discrepancies of the same order and of both signs. Obviously only a small error in the amplitude or device slope measurements will move the calculated intersection considerably. Moreover it is not known how the weak function $\bar{Y}(\omega)$ alters the theoretical sideband condition.

5.4 *Further Observations*

Hysteresis between locking-in and unlocking frequencies was observed even with double-tuned circuits, usually where the load-line is most inclined to the vertical. The effect is ascribed to the second-order effect of amplitude variations, and is such that more power is required to pull-in an unlocked oscillator than to maintain locking at the same frequency.

Low-frequency switching between two states was found for some critical adjustments of a triple-tuned circuit in which two loop-type resonances interfere. The time-constant was associated with that of build up and decay of oscillations in the circuit.

The oscillator could be pulled by a small injected signal, when the frequencies were widely different but the circuit admittances similar, as by the cross-over of a loop.

Where spurious sidebands were present, locking of the whole pattern occurred whenever the driver was close to any of the sidebands.

VI. CONCLUSION

Measurements on a low-frequency lumped circuit model have substantiated earlier theory[5] concerning the interaction of a negative admittance and a multi-resonant circuit. The model described is not capable of simulating devices whose characteristics are more complicated than the simple form $\bar{Y}(A)$. For example, it is not easy to duplicate with lumped elements the observations which have been made on microwave oscillators, involving generation of the *same* frequency at two different diode bias currents, or utilizing second-harmonic tuning or sub-harmonic pumping.

However the experiment shows that many of the complex phenomena associated with tuning of solid-state microwave oscillators may be reproduced under these simplified conditions, and that therefore it is very frequently the microwave circuit, rather than the device, which is at fault. In addition, the practicability of broad-banding circuits for deviator and locking-amplifier applications has been demonstrated.

VII. ACKNOWLEDGMENT

The author wishes to acknowledge the advice and encouragement of K. Kurokawa in this work.

REFERENCES

1. Van der Pol, B., "Forced Oscillations in a Circuit with Nonlinear Resistance," *Phil. Mag., 3* (1927), pp. 65–80.
2. Minorsky, N., *Nonlinear Oscillations,* Princeton, N. J.: D. Van Nostrand Co., Inc., 1962.
3. Khokhlov, R. V., "A Method of Analysis in the Theory of Sinusoidal Self-Oscillations," *IRE Trans. Circuit Theory, CT-7,* No. 4 (December 1960), p. 398.
4. Adler, R., "A Study of Locking Phenomena in Oscillators," *Proc. IRE, 34,* No. 6 (June 1946), p. 351.
5. Kurokawa, K., "Some Basic Characteristics of Broadband Negative Resistance Oscillator Circuits," *B.S.T.J., 48,* No. 6 (July 1969), pp. 1937–1955.